



Direct and indirect impacts of land use/cover change on urban heat environment: a 15-year panel data study across 365 Chinese cities during summer daytime and nighttime

Tong He · Nan Wang · Jiayue Chen · Feng Wu · Xinliang Xu · Luo Liu · Dongrui Han · Zongyao Sun · Yingshuang Lu · Yan Hao · Zhi Qiao

Received: 16 May 2023 / Accepted: 19 October 2023 / Published online: 6 March 2024
© The Author(s) 2024

Abstract

Context Land use/cover change (LUCC) can directly and indirectly affect surface urban heat island intensity (SUHII) and the effects need to be decomposed.

Objectives To perform long-term trend analyses of contribution indexes (CIs) of land use types to urban heat environment in cities and to deconstruct direct and indirect effects of LUCC on SUHII within geographical regions.

Methods Mann–Kendall test and Sen’s slope were used to examine the trends of CIs and SUHII in 365 cities during summer of 2005–2019. Structural equation models were established to quantify direct and indirect effects of land use types’ CIs on SUHII in six geographical regions of China.

Results First, SUHII in 78.08% and 73.70% of the Chinese cities increased during summer daytime and nighttime, respectively. Second, the CI of built-up land significantly increased across more than half of the cities in all the six regions. Third, not all land use types exerted both direct and indirect effects on SUHII. At daytime, the CI of cropland (direct) was the dominant factor in East China (1.386),

Supplementary Information The online version contains supplementary material available at <https://doi.org/10.1007/s10980-024-01807-1>.

T. He · N. Wang · J. Chen · Y. Lu · Z. Qiao (✉)
School of Environmental Science and Engineering, Tianjin University, Tianjin 300350, China
e-mail: qiaozhi@tju.edu.cn

T. He · Y. Hao
School of Environment, Beijing Normal University, Beijing 100875, China

F. Wu
Institute of Geographical Sciences and Natural Resources Research, Chinese Academy of Sciences, Beijing 100101, China

X. Xu
State Key Laboratory of Resources and Environmental Information Systems, Institute of Geographical Sciences and Natural Resources Research, Chinese Academy of Sciences, Beijing 100101, China

L. Liu
Guangdong Province Key Laboratory for Land Use and Consolidation, South China Agricultural University, Guangzhou 510642, China

D. Han
Institute of Agricultural Information and Economics, Shandong Academy of Agricultural Sciences, Jinan 250100, China

Z. Sun
School of Architecture, Tianjin University, Tianjin 300272, China

South-central (-0.637), and Northwest (-0.399) regions. At nighttime, the CI of water bodies (both direct and indirect) was the dominant factor in Northwest (0.506) and Northeast (0.697) regions while CI of built-up land (both direct and indirect) determined in North China (0.476).

Conclusions Separation of direct and indirect effects of land use types on SUHII had practical implications for cities to optimize the structures and functions of ecosystems and to take regionally based actions improving the urban heat environment.

Keywords Urban heat environment · Land use/cover change · Contribution index · Regional climate · Direct and indirect impacts

Introduction

Cities are the engine and driving force of social development in today's rapidly urbanizing world, providing living spaces for the growing global population (Oke et al. 2017). In recent years, however, the deterioration of urban heat environment (UHE) in cities has become increasingly salient, e.g. the urban heat island effect whereby temperatures in urban areas are higher than those in surrounding suburban or rural areas (Yang et al. 2019; Qiao et al. 2023a, b). The urban heat island has been observed in numerous countries and regions worldwide, resulting in air pollution, energy consumption, and human health outcomes (Qiao et al. 2020; He et al. 2022; Hou et al. 2022). A series of changes in UHE cannot be separated from land use/cover change (LUCC; Hu et al. 2017; IPCC 2021). Because the conversion of land use types and surface processes can change the biophysical parameters that determine energy absorption and partition, resulting in unfavorable outcomes for human habitation generated in UHE (Fu and Weng 2016; Huang et al. 2018; Chen et al. 2019). Therefore, in order to achieve the Sustainable Development Goal (SDG) 11 of "make cities and human settlements inclusive, safe, resilient and sustainable" proposed by United Nations, it is necessary to analyze the UHE from the perspective of LUCC (UN 2018; He et al. 2022). Guided by ecological knowledge and landscape sustainability theory, cities and regions are able to unleash their potential for operability

and effectiveness in sustainable implementation and development (Wu 2013).

Previous studies have extensively explored the impact of LUCC on UHE (Zhou et al. 2014; Hu et al. 2017; Huang et al. 2018; Xiao et al. 2018), and the contribution index (CI) of land use types or landscapes to UHE has been investigated. Chen et al. (2006) proposed the CI of land use type to UHE, and it reflects the impacts of both the LST and area from a specific land use type on UHE. Since then, CI has been widely used to quantify the warming and cooling effects of land use types on UHE (Qiao et al. 2013). Comparison of CIs in different cities shed light on cities' growth states and expansion patterns (Lu et al. 2015; Tarawally et al. 2018; Huang et al. 2019). At the same time, Xu (2009) utilized CIs to refine the source and sink theory in UHE studies by clarifying the roles that different landscapes play. Additional exploration of the impacts of landscape composition and configuration on UHE in terms of source and sink laid a foundation for proposals aimed at improving UHE (Ayanlade and Jegede 2015). Nonetheless, it is imperative to note that the majority of these investigations predominantly focused on calculating the CI of specific land use types or merely classifying certain land areas as source or sink landscapes within specific cities, often within a limited temporal context. Consequently, while previous studies have significantly advanced our understanding of UHE and its relationship with land use types, a substantial gap has emerged in the literature. To address this deficiency, there is a pressing need for a comprehensive and longitudinal analysis of all land use types' CIs at a national scale. Such an endeavor would facilitate the identification of sources and sinks of UHE, the assessment of their evolving dynamics, and the enhanced comparative analysis among diverse cities.

The land system architecture configurations based on geospatially explicit LUCC contribute to the landscape and regional sustainability (Wu 2019). As a measure of landscape and regional sustainability, UHE is also the response to various combinations and configurations of land use types and patterns, rather than being determined by a single land use type alone (Xiao et al. 2018; Huang et al. 2019). In a city, an increase in the area of a particular land use type usually means a reduction of other land use types (Chen et al. 2020; Zhou et al. 2020). Simultaneously, one land use type is

capable of affecting the LST of a neighboring land use type and further the entire city's LST, thus completely altering the CIs of all land use types (Huang et al. 2019; Zawadzka et al. 2021). This underscores the fact that each land use type exerts not only its own contribution to UHE but also indirectly affects the contributions of other land use types to UHE. Remarkably, previous research endeavors have often overlooked this indirect effect, thereby warranting further investigation. The quantification of both direct and indirect impacts of CIs associated with various land use types on surface urban heat island intensity (SUHII) is of paramount significance for urban sustainable development. Importantly, it is essential to acknowledge that the influence of landscapes on local climate patterns is inherently tied to geographical specificity (Cao et al. 2021). Hence, to gain a comprehensive understanding of LUCC's contribution to SUHII, it is imperative to transcend the confines of a single city and account for spatial variations. It becomes necessary to include cities situated in diverse geographical regions within the research purview to discern and elucidate the spatial differences in the interplay between LUCC and SUHII.

The present study aims to explore the spatiotemporal patterns of land use types' CIs and their complex effects on SUHII. Based on 365 Chinese cities, this study attempts to address the following scientific questions: (i) how did the CIs of land use types to UHE change in a long time series, and (ii) how did land use types directly and indirectly affect the SUHII in different regions. Direct and indirect impacts can be distinguished using structural equation modeling (SEM; Wu et al. 2021). This study performed SEM to assess the impact of CIs on SUHII for all cities in the same region, in a bottom-up approach aimed at expanding the city-scale heat environment indexes to the complex effect clarification at regional scale. The findings will advance our understanding of long-term changes in the effects of land use types on UHE and interactions between the different land use types. Knowledge of the ecological functions fulfilled by land use types, scientific land use optimization, territorial spatial planning, and urban renewal can reduce the negative effects of UHE, provide ecological knowledge-based support for urban sustainable development, and inform actions aimed at mitigating climate change.

Study area

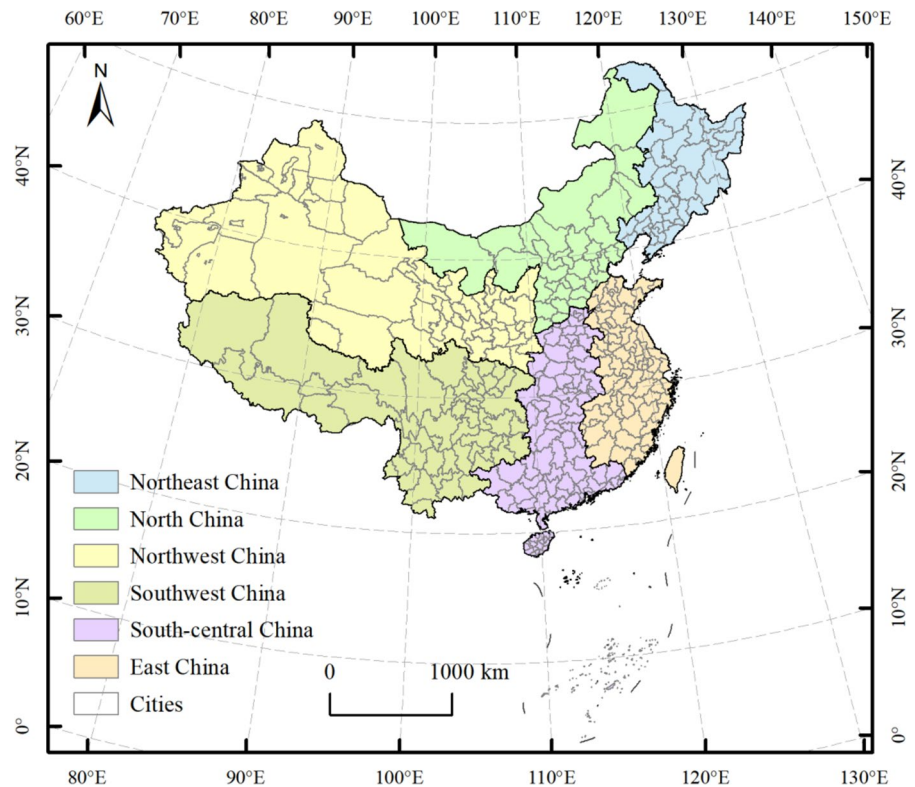
As the world's largest developing country, China has a vast territory with numerous cities at different developmental stages. In China, the relationship between humans and nature is a key factor in the construction of ecological civilization. Crucial aspects in this regard include coordinated optimization of regional land use and sustainable development of cities. Urbanization in China entered a period of particularly rapid growth from 2005 onwards, and a wide range of land use policies have been implemented accordingly in recent years (Xi et al. 2022; Qiao et al. 2023a). Consequently, China emerges as an exceptionally compelling focal area for in-depth investigation. This study included 365 prefecture-level administrative cities in China, without Hong Kong, Macau, Taiwan Province, Sansha City of Hainan Province, Zhoushan City of Zhejiang Province because of the unavailability of certain data in the dataset. In view of the great differences in natural conditions among the cities, they were divided into six regions based on their geospatial locations, i.e., Northeast China (NE), North China (NC), Northwest China (NW), Southwest China (SW), South-central China (SC), and East China (EC) (Fig. 1).

Data and methods

Data

LST data were derived from version 6 (V6) of the MODIS 8-day Level 3 global MYD11A2 product, with a spatial resolution of 1 km (<https://ladsweb.modaps.eosdis.nasa.gov>). The Aqua satellite was launched in July 2002, and the data that it has retrieved have stabilized since 2005. LST was retrieved using the split-window algorithm under clear-sky conditions. The current version (V6) of MODIS LST data has improved the algorithm and thus the accuracy and stability of the data (Wan 2014). The accuracy assessment of the V6 product showed that the mean LST error was within 0.6 K (Wan 2014). The MYD11A2 product was acquired at 13:30 p.m. and 01:30 a.m. (local solar time), representing the available intraday maximum and minimum LST, respectively. To investigate the CIs of land use types in summer daytime and nighttime, the

Fig. 1 The 365 cities and 6 geographical divisions of China examined in this study



mean LSTs at 13:30 p.m. and 01:30 a.m. from June to August during the period 2005–2019 were calculated. The quality control (QC) dataset attached to the product was used to exclude low-quality pixels affected by clouds or other factors, and pixels with average LST error ≤ 2 K (QC flag is “00” or “01”) were included in subsequent analysis. Projection transformation, data extraction, quality control, and data calculations were carried out using the Google Earth Engine (GEE).

LUCC was derived from the annual global product of the European Space Agency’s Climate Change Initiative Land Cover project (<http://maps.elie.ucl.ac.be/CCI/viewer/index.html>). This dataset has been widely used to detect global land use/land cover changes, with an overall accuracy of 75.4% (UCL-Geomatics 2017; Mousivand and Arsanjani 2019). The LUCC data from 2005 to 2019 were obtained. The spatial resolution of the original data was 300 m, which were resampled to 1 km using the “nearest” technique, in order to correspond to the spatial resolution of the remaining data. In this study, we incorporated the original subcategories into 6 categories (i.e., cropland, forest, grassland, water bodies, built-up land, and bare land) for the subsequent analysis.

Resampling and reclassification of LUCC were performed using the ArcGIS 10.3 platform.

DEM was obtained from the Resource and Environment Science and Data Center of Chinese Academy of Sciences (<http://www.resdc.cn>), derived from the Shuttle Radar Topography Mission data with a 1-km spatial resolution.

Methods

First, we calculated the CIs of six land use types and SUHII in each city in summer daytime and nighttime from 2005 to 2019, using LST, LUCC, and DEM data. Second, we performed trend analysis for the CIs of six land use types and SUHII in the 15-year continuous temporal coverage (2005–2019), using the MK test and Sen’s slope estimator. Finally, the structural equation models were constructed of the CIs and SUHII in 2019 to explore the complex effects (including direct and indirect paths) of different land use types on SUHII for cities located in different geographical regions. This study’s technical roadmap is shown in Supplementary Fig. S1.

CI of land use types to UHE

The CI of each land use type to UHE was defined as:

$$CI = (\overline{LST}_i - \overline{LST}) \times \frac{S_i}{S}, \tag{1}$$

where \overline{LST}_i is the mean LST of the i th land use type and \overline{LST} is the mean LST of the entire city (K); S_i is the area of the i th land use type and S is the area of the entire city; i is the number of land use types (1, cropland; 2, forest; 3, grassland; 4, water bodies; 5, built-up land; 6, bare land). CI is positive when $(\overline{LST}_i - \overline{LST})$ is positive, indicating a warming contribution of a specific land use type to UHE. CI is negative when $(\overline{LST}_i - \overline{LST})$ is negative, indicating a cooling contribution of a specific land use type to UHE. Based on the preprocessed summer daytime/nighttime mean LSTs and the LUCC data, the CIs of six land use types in each city to the summer daytime and nighttime UHE were calculated from 2005 to 2019.

SUHII

The SUHII was defined as the LST difference between the city itself and the background field (Zhou et al. 2019):

$$SUHII = \frac{1}{n} \sum_{j=1}^n (LST_j - \overline{LST}_{background}) \text{ if } LST_j > \overline{LST}_{background}, \tag{2}$$

where LST_j is the LST of the j th pixel and $\overline{LST}_{background}$ is the mean LST of the background field. Pixels 50 m higher than the median DEM of the city were excluded given the sensitivity of LST data to elevation (Wu et al. 2021). Then, the background field (the land use types of cropland, forest, grassland and bare land) was extracted and the mean LST of the background field ($\overline{LST}_{background}$) was calculated. Accordingly, pixels in the city whose LSTs were larger than $\overline{LST}_{background}$ can be enumerated by j (from 1 to n). Finally, the mean positive difference between the LSTs of all pixels in the city and $\overline{LST}_{background}$ was calculated as the city's SUHII (K). The summer daytime and nighttime SUHIIs for each city were obtained during the period 2005–2019.

Trend analysis

The Mann–Kendall (MK) test is a rank-based non-parametric method for estimating trends in time series data. It tolerates outliers and is applicable to all data distribution types (Hou et al. 2022). For known time series data $X(x_1, x_2, x_3, \dots, x_n)$, the statistical significance of the MK test is expressed using the statistic s :

$$s = \sum_{i=1}^{n-1} \sum_{j=i+1}^n \text{sgn}(x_j - x_i), \tag{3}$$

where n is the sample size; x_j and x_i represent the sample data values for the j th and i th terms ($j > i$), respectively; the sign function $\text{sgn}(x_j - x_i)$ is $-1, 0,$ and 1 for $(x_j - x_i) < 0, = 0,$ and $> 0,$ respectively. The variance of the statistic s was calculated as follows:

$$\text{Var}(s) = \frac{n(n-1)(2n+5) - \sum_{p=1}^q t_p(t_p-1)(2t_p+5)}{18}, \tag{4}$$

where t_p is the amount of data in the p th binding group, and q is the number of binding groups. A binding group was a set of sample data with the same value given that there may be multiple sample data-points. The normalized test statistic Z was calculated using the statistic s and its variance $\text{Var}(s)$:

$$Z = \begin{cases} \frac{s-1}{\sqrt{\text{Var}(s)}} & \text{if } s > 0, \\ 0 & \text{if } s = 0, \\ \frac{s+1}{\sqrt{\text{Var}(s)}} & \text{if } s < 0. \end{cases} \tag{5}$$

The positive (negative) value of Z indicates the increasing (decreasing) trend in the time series data. The MK test assumes that there is no significant monotonic trend (null hypothesis, H_0). At a given α confidence level, the typical normal distribution table states that the H_0 is statistically rejected when $|Z|$ is greater than $Z_{1-\alpha/2}$, indicating a significant monotonic trend. By contrast, the H_0 is accepted when $|Z|$ is not greater than $Z_{1-\alpha/2}$, indicating an insignificant trend. The MK test has been widely used to explore trends and patterns of urban heat island intensity and LST in relation to the UHE (Wu et al. 2021; Hou et al. 2022). Simultaneously, the MK test is typically combined with the Sen's slope estimator to indicate the speed of change. The Sen's slope estimator is effective because it is not

influenced by an extreme distribution or missing data. The magnitude of the trend slope for a given item of time series data is calculated as follows:

$$\beta = \text{median}\left(\frac{x_j - x_i}{j - i}\right), \quad (6)$$

where x_j and x_i are the sample data values for the j th and i th terms ($j > i$), respectively; β represents the slope value of the time series sample per unit time, which is indicated by the median of the slopes of all data pairs.

In the present study, the MK trend test and Sen's slope estimator were applied to detecting the trends of CIs and SUHII in 365 Chinese cities during the period 2015–2019 at a significance level α of 0.05 (95% confidence level of significance). The above processes were carried out in Python with pyman-kendall package (version 1.4.2).

Structural equation modeling

The structural equation modeling (SEM) can establish, estimate, and describe causal relationships among multiple factors; in particular, it can quantify direct and indirect effects in causal networks (Lang et al. 2018). SEM assumes excellent data–model fit, but the test results will statistically reject the original hypothesis when significant paths are not considered. Model fit is evaluated by the following goodness-of-fit indexes: p -value of the entire model > 0.05 ; comparative fit index (CFI) or Tucker–Lewis index (TLI) close to 1; root mean squared error of approximation (RMSEA) < 0.05 ; standardized root mean square residual (SRMR) < 0.06 ; goodness of fit index (GFI) close to 1 (Xiang et al. 2022).

The CIs of land use types not only directly affect SUHII, but also have mutual feedbacks between land use types, thus the CIs are likely to have indirect effects on SUHII (Supplementary Fig. S2). The Pearson correlation analysis of the summer daytime and summer nighttime CIs and the SUHII in 2019 was performed first for the six regions, laying a foundation for identifying interrelationships in the SEM. We added possible causal relationships between two variables with significant correlations, and adjusted the SEMs by increasing or decreasing causal connections continuously according to fitting results. Using the lavaan package (version 0.6) in the R software, the

models were fitted until the goodness-of-fit indexes were achieved. Standardized path coefficients were used to quantify the direct and indirect effects of CIs on SUHII. The total effects of each land use type's CI on the city-scale SUHII within the same region were the sum of direct and indirect effects.

Results

Change of SUHII from 2005 to 2019

From 2005 to 2019, summer daytime SUHII exhibited an increasing trend ($0.0288 \text{ K year}^{-1}$, the mean Sen's slope) in 285 cities (78.08%), 153 of which showed a significant increase. Meanwhile, 80 cities (21.92%) showed a decrease ($-0.0178 \text{ K year}^{-1}$) in SUHII, 8 of which showed a significant decrease. In summer nighttime, SUHII exhibited an increasing trend ($0.0097 \text{ K year}^{-1}$) in 269 cities (73.70%), 80 (21.92%) of which showed a significant increase; meanwhile, SUHII decreased ($-0.0045 \text{ K year}^{-1}$) in 96 cities (26.30%), 4 (1.10%) of which showed a significant decrease (Fig. 2).

For summer daytime, the NW region had the widest range of SUHII slopes (-0.1074 to $0.1369 \text{ K year}^{-1}$), with 71.93% and 28.07% of cities showing increasing and decreasing trends of SUHII, respectively, and the NW region witnessed the largest percentage of cities with significant decreasing in SUHII (8.33%). The NE and NC regions had a similar range of SUHII slopes (-0.0329 to $0.0561 \text{ K year}^{-1}$ and -0.0413 to $0.0601 \text{ K year}^{-1}$, respectively), with 55.88% and 65.71% of cities exhibiting increasing SUHII, respectively. The SW, SC and EC regions all witnessed an SUHII increase in more than three-quarters of cities (77.36%, 88.88%, and 96.05% of cities, respectively). In the EC region in particular, 72.37% of cities witnessed a significant increase in SUHII, and cities with large slopes formed clusters in the eastern part of the region.

Compared with summer daytime, the distribution of the slopes during summer nighttime was more compact, and the speed at which SUHII changed at night was lower than that during the daytime. Moreover, the proportions of cities with significant increases in SUHII in each region were substantially lower than that during the daytime. The nighttime SUHII slope was most

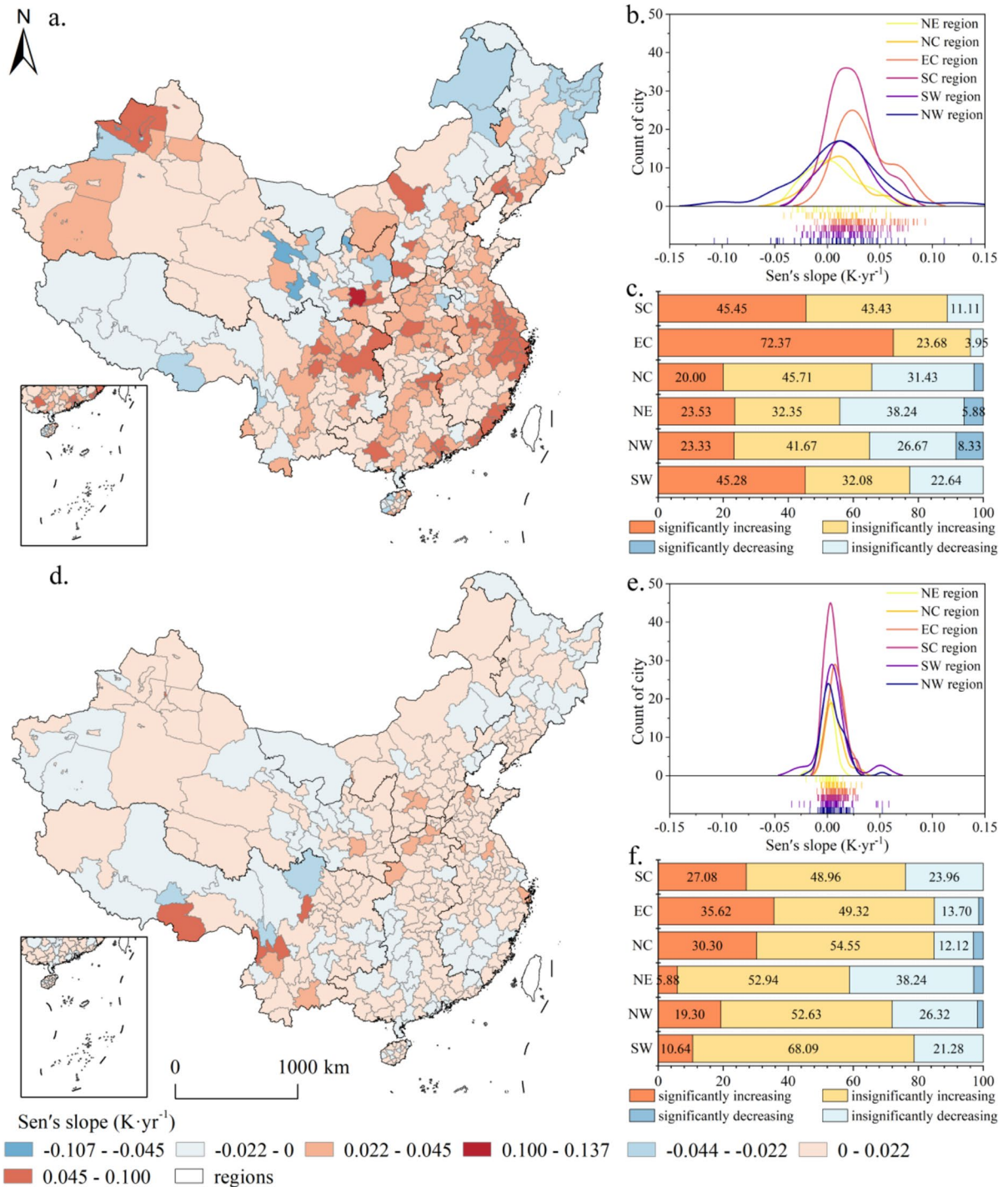


Fig. 2 Changes in SUHII from 2005 to 2019 in summer daytime and nighttime (95% confidence level of significance): **a–c** in summer daytime, **d–f** in summer nighttime, **a** and **d** Sen's slope of SUHII, **b** and **e** plots of Sen's slope (whiskers below the horizontal axes indicate that the corresponding Sen's

slopes appear), and **c** and **f** percentage (%) of cities with different trends of SUHII in each region; only cities with significant or insignificant change trends were considered in the statistical analysis

widely distributed in the SW region (-0.0340 to 0.0587 K year⁻¹), and 78.73% of cities in the SW region had an increase in SUHII. The proportions of cities with increasing SUHII in the EC and NC regions were 84.94% and 84.85%, respectively. The EC region also peaked in the proportion of significantly increased cities (35.62%).

Spatiotemporal changes of CIs of land use types

Spatial variability of CIs of land use types

In 2019, considerable spatial variability of the land use types' CIs to UHE was found, and the CIs of some land use types were spatially linked (Fig. 3). In both of the summer daytime and nighttime, the CIs of forest were low in cities with high CIs of cropland, especially during the daytime. The CIs of grassland in the NW region were mostly negative, forming aggregations with a large cooling effect in its western part; conversely, the CIs of bare land in the NW region were prominently positive. During summer daytime, cropland showed a negative CI to UHE in 24.66% of cities while a positive CI to UHE in 75.34% of cities. The proportion of cities with a positive CI of water bodies was 25.76%; however, these positive water bodies' CIs and the areas of water bodies were small. The proportion of cities with a positive CI of built-up land reached 92.86%, with high positive CIs of built-up land clustered in the Pearl River Delta and Yangtze River Delta urban agglomerations and the remainder being primarily distributed in provincial capitals and municipalities. For some cities within the NW and NC regions, however, built-up land produced a negative CI. During summer nighttime, cropland showed a negative CI to UHE in 35.07% of cities while a positive CI to UHE in 64.93% of cities. The proportion of cities with a positive CI of water bodies reached 93.43%, which was largely higher than that during the daytime. A positive CI of built-up land was observed in 96.71% of cities.

Changes in CIs of land use types from 2005 to 2019

The speed of change (Sen's slopes) of the CIs for each land use type differed spatially. The higher the value of Sen's slopes (either positive or negative),

the faster the change speed of CIs (either increasing or decreasing). And the trends differed by region (Figs. 4, 5; Supplementary Fig. S3; Supplementary Tables S1–S12). In the daytime, except the EC and NE regions, more than half of the cities in other regions showed increasing trends of CI of cropland. The EC region showed the highest percentage of cities with a significant decreasing trend of CI of cropland (34.67%), followed by the NE region (27.78%). The cities with a prominent positive slope for CI of cropland were concentrated in the Beijing–Tianjin–Hebei and Chengdu–Chongqing urban agglomerations. All regions showed a decrease in CIs of both forest and grassland in more than half of the cities, especially the EC region (71.23% for forest and 67.11% for grassland). The cities with significantly increasing and decreasing trends of CI of water bodies peaked in the NW (23.21%) and NC (26.47%) regions, respectively. And the cities with prominent negative slopes for CI of water bodies were distributed in the EC region. More than half of the cities in all regions exhibited significant increases in the CI of built-up land, with all cities in the SC and EC regions showing an increasing trend. The SW region showed the highest percentage of cities with a significant increase in the CI of built-up land (96.30%), while the CI decreased significantly in 26.67% of cities in the NW region. Absolute values of positive slopes for CI of built-up land were higher than those of negative slopes, indicating that the change speed was significantly higher in cities with increasing CI of built-up land. The cities with high positive slopes were clustered in the Beijing–Tianjin–Hebei, Chengdu–Chongqing, Pearl River Delta and Yangtze River Delta, and Yangtze River Delta urban agglomerations. Only the SW region had more cities with an increasing (73.81%) trend of CI of bare land, while the remaining five regions had more than half of cities showing a decreasing trend.

In the nighttime, the range of Sen's slopes for CIs of all land use types was relatively narrow, indicating that the speeds of changes in CIs were slower than in the daytime. CI of cropland in > 50% of the cities showed a decreasing trend in all regions except the NE; and in the NC and SW regions, no significant increases in the CI of cropland were observed. The cities with prominent positive slopes for CI of cropland were distributed in the NW and EC regions. The EC region witnessed the highest percentage of cities

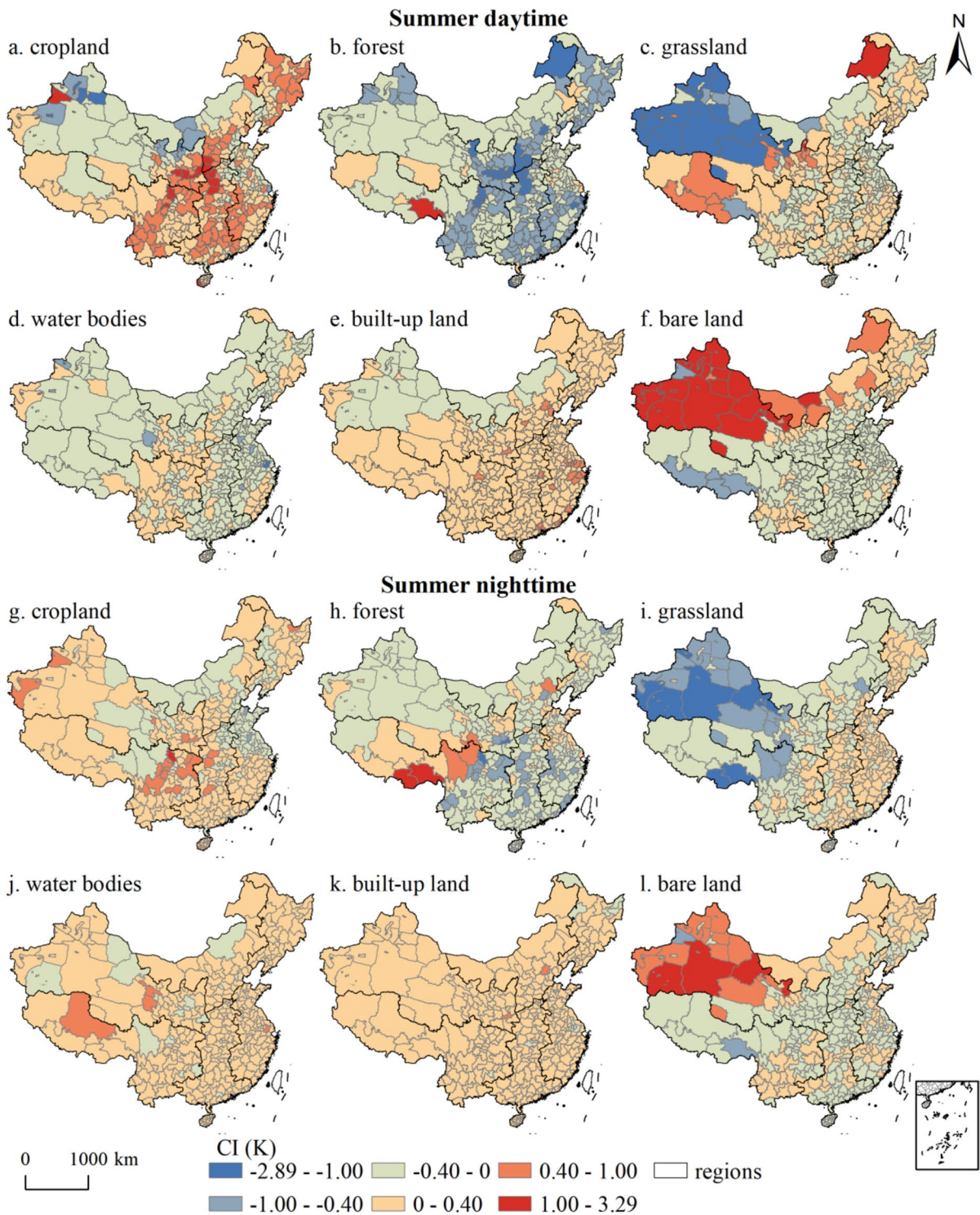


Fig. 3 The CIs of land use types to UHE in 2019 in summer daytime and nighttime

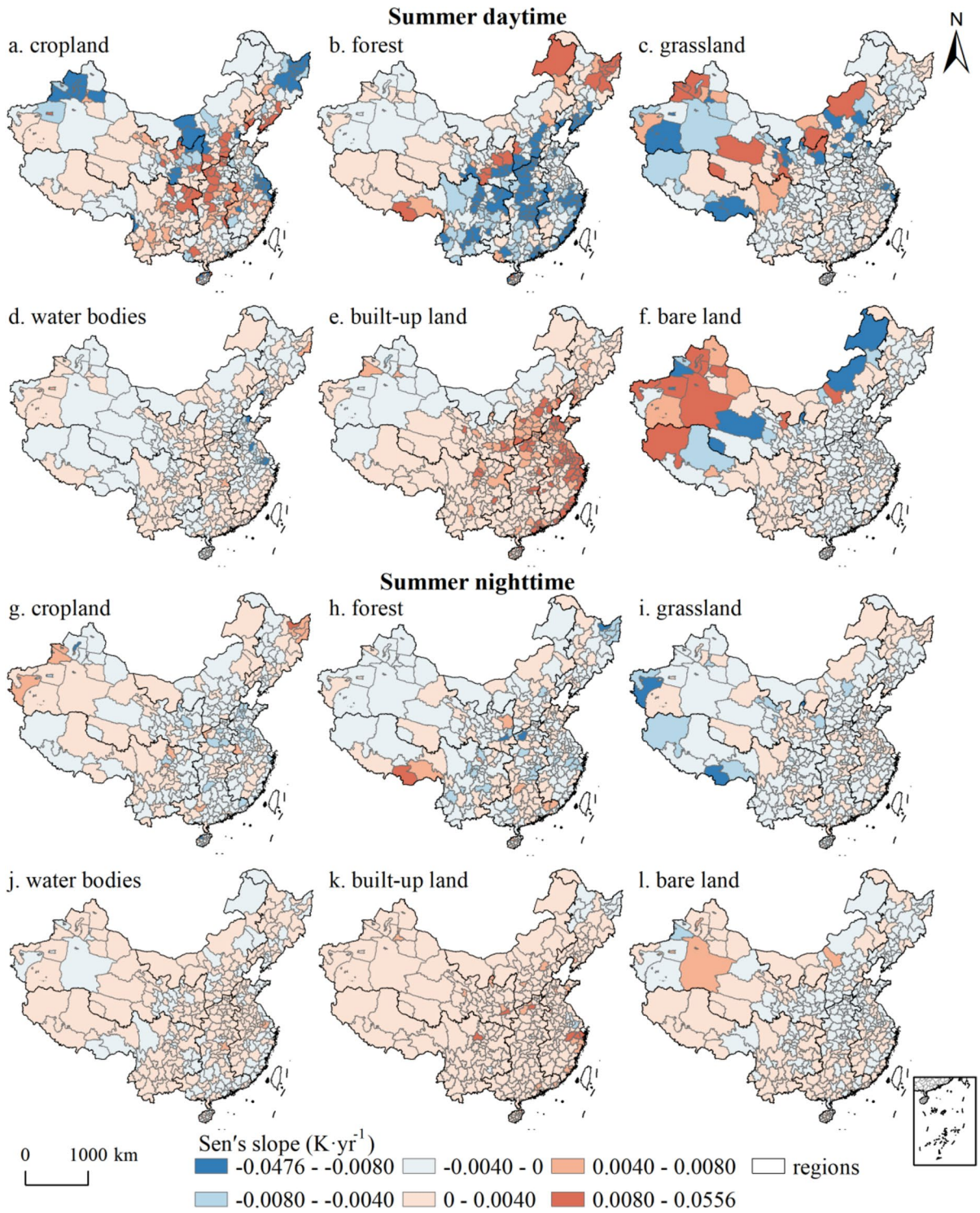


Fig. 4 Sen's slope of CIs of land use types to UHE from 2005 to 2019 in summer daytime and nighttime (95% confidence level of significance)

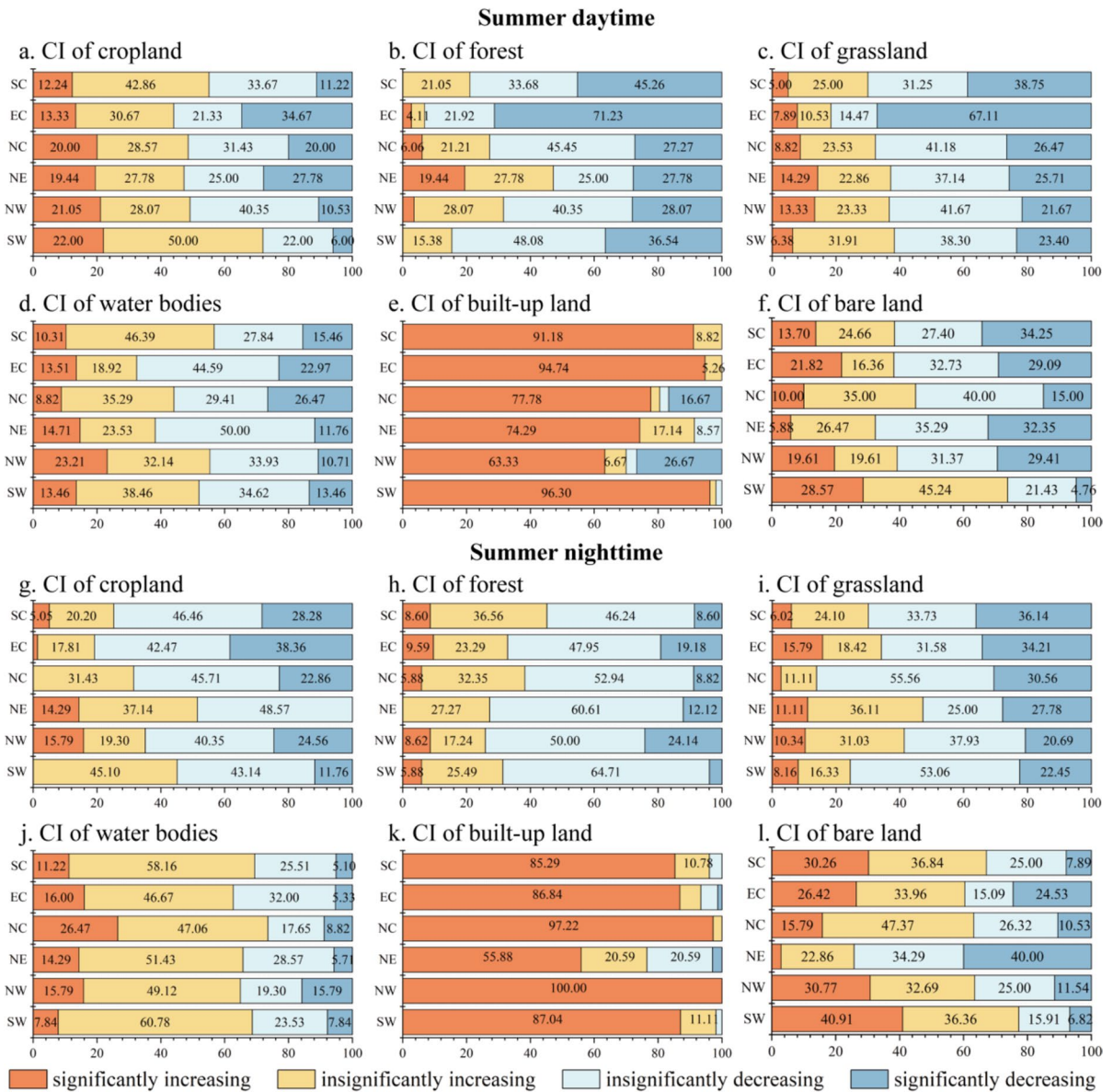
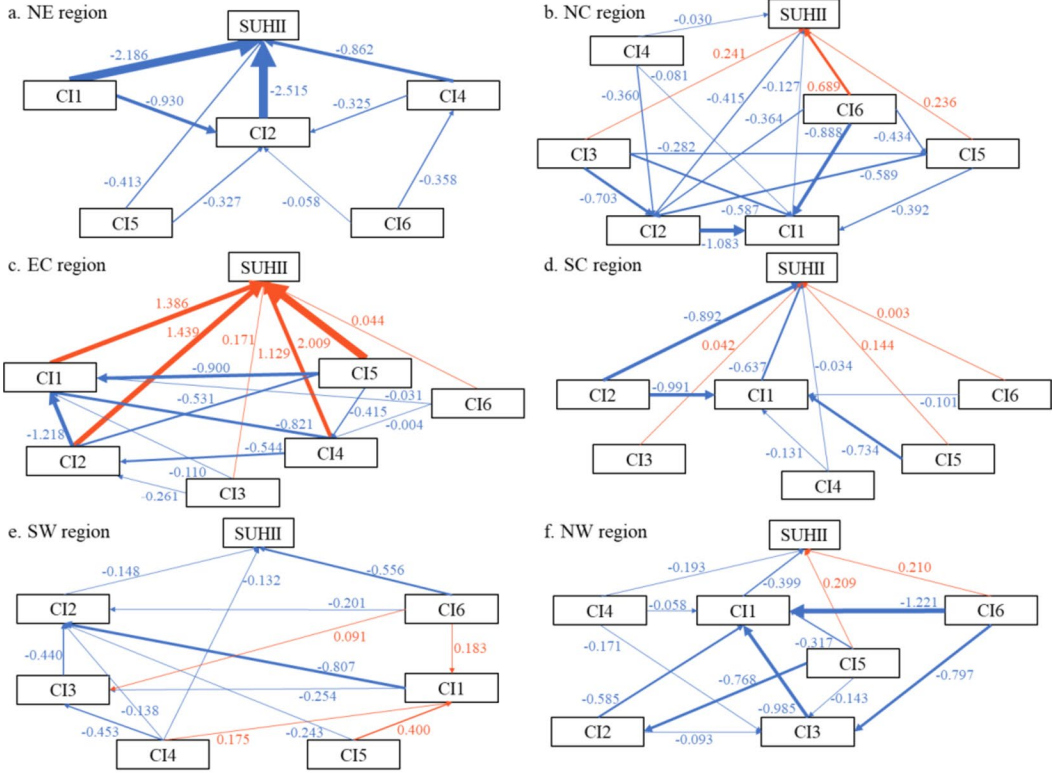


Fig. 5 Percentage (%) of cities with different trends of CIs of land use types to UHE in each region from 2005 to 2019 in summer daytime and nighttime. Only cities with significant or insignificant change trends were considered in the statistical analysis

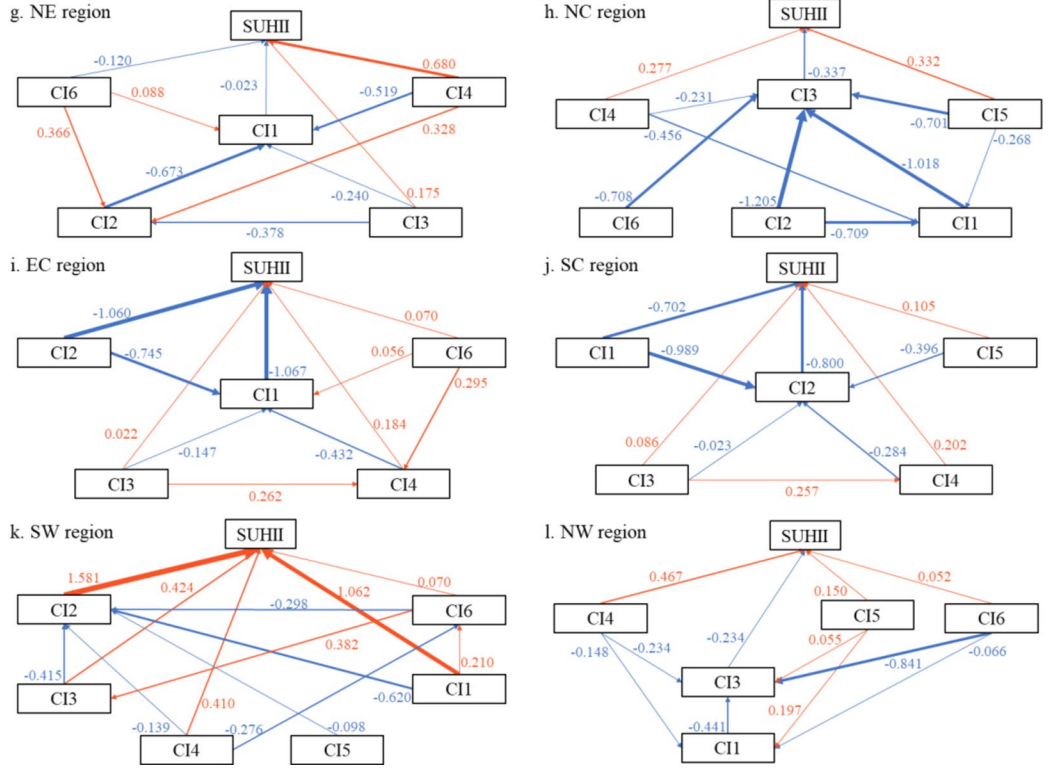
with significant increases in CIs of forest and grassland, i.e., 9.59% and 15.79% respectively. In the NW region, the CI of forest showed a decreasing trend in 74.14% of cities, with a significantly decreasing trend observed in 24.14% of cities. And the cities showing prominent positive slopes for CI of forest were located mostly in the SW and SC regions. In the NC region, the CI of grassland showed a decreasing trend in 86.12% of cities. More than 50% of the cities in

all regions showed an increasing trend of CIs of water bodies and built-up land. In particular, 73.53% of the cities in the NC region showed an increase in CI of water bodies, and all cities in the NC and NW regions showed an increase in CI of built-up land. The SW region had the highest percentage of cities with an increasing trend in CI of bare land (77.27%), whereas the NE region had the highest percentage of cities with a decreasing trend in CI of bare land (74.29%).

Summer daytime



Summer nighttime



◀Fig. 6 The structural equation models of CIs of land use types and SUHII in six regions in summer daytime and nighttime. *Arrows indicate the direction of causality, with the orange lines showing positive effects and the blue lines showing negative effects. Numbers on the lines are the standardized path coefficients. Numbers adjacent to CIs represent land use types, 1: cropland; 2: forest; 3: grassland; 4: water bodies; 5: built-up land; 6: bare land

Direct, indirect, and total effects of CIs on SUHII

The correlations among CIs of land use types and SUHII in 2019 showed significant regional differences (Supplementary Fig. S4). Based on the correlations among CIs of land use types and SUHII, the SEMs were established to understand the effects of CIs of land use types on SUHII for the six regions in summer daytime and nighttime. The goodness-of-fit indexes of the SEMs indicated that all models could explain the causative relationship (Supplementary Table 13). The 365 Chinese cities were located in regions with different configuration of land use types, which had a substantial impact on the results of the SEM assessment (Figs. 6, 7).

In the NE region, all pathways showed negative effects in the daytime, with the CIs of forest (-2.515 , the path coefficient) and cropland (-2.186) exhibiting the most direct effects on SUHII. However, the CI of cropland also had an indirect effect (2.339) through CI of forest on SUHII, resulting in a total effect of only 0.153 . In the nighttime, only a direct effect was observed on SUHII from the CI of cropland, with CIs of forest, grassland, water bodies, and bare land all exhibiting indirect effects via the CI of cropland.

In the NC and EC regions, the CI of cropland only exerted a direct effect on SUHII in the daytime, while the CIs of the remaining five land use types exhibited both direct and indirect effects. In the NC region, the CIs of forest, grassland, water bodies, built-up land, and bare land influenced SUHII through the CI of cropland in the daytime. In the nighttime, the CI of grassland only exerted a direct effect (-0.337), while the CIs of cropland, forest, water bodies, built-up land, and bare land all exhibited indirect effects on SUHII through the CI of grassland. The direct effect from the CI of built-up land (0.332) and its indirect effect through the CIs of cropland and grassland (0.144) resulted in a total effect on SUHII of 0.476 .

In the EC region during the daytime, the CIs of forest, grassland, water bodies, built-up land, and bare

land all influenced SUHII through the CI of cropland. The direct effects from CIs of all land use types on SUHII were positive, while the pathways among CIs were negative. The direct effects from CIs of built-up land and forest were positive (2.009 and 1.439 , respectively), whereas the indirect effects from them were negative (-1.168 and -1.688 , respectively). Thus, the total effects from CIs of built-up land and forest after offsetting were 0.841 and -0.249 , respectively. In the nighttime, the CIs of cropland and forest had negative direct effects on SUHII, while the CIs of grassland, water bodies, and bare land produced positive direct effects on SUHII. The CIs of forest, grassland, water bodies, and bare land all exerted indirect effects on SUHII through the CI of cropland.

In the SC region, the CIs of cropland (-0.637) and grassland (0.042) only produced direct effects on SUHII in the daytime, while the CIs of the remaining four land use types exerted both direct and indirect effects, all of which indirectly affected SUHII through the CI of cropland. In the nighttime, the CIs of cropland and forest had negative direct effects on SUHII, while the CIs of grassland, water bodies, and built-up land had positive direct effects on SUHII. The CIs of cropland, grassland, water bodies, and built-up land all had indirect effects on SUHII through the CI of forest. The direct effect (0.202) and indirect effect (0.227) from the CI of water bodies resulted in a total effect on SUHII of 0.429 .

In the SW region, the CI of forest exerted only a direct effect (-0.148) on SUHII in the daytime, while the CIs of cropland (0.103), grassland (0.065), and built-up land (0.077) exerted only indirect effects. The CIs of water bodies and bare land exerted both direct and indirect effects. In the nighttime, the CIs of cropland, forest, grassland, water bodies, and bare land all exerted positive direct effects on SUHII, with the direct effect from CI of forest peaking at 1.581 . The CI of built-up land exerted only an indirect effect (-0.155) on SUHII through the CI of forest.

In the NW region, the CI of cropland affected SUHII only through a direct pathway (-0.399), with CIs of forest (0.197) and grassland (0.393) exerting effects only through indirect pathways in the daytime. Meanwhile, the CIs of water bodies (-0.237), built-up land (0.128), and bare land (0.384) exerted both direct and indirect effects on SUHII. In the nighttime, only a direct effect of the CI of grassland on SUHII was observed, and the CI of cropland only exerted

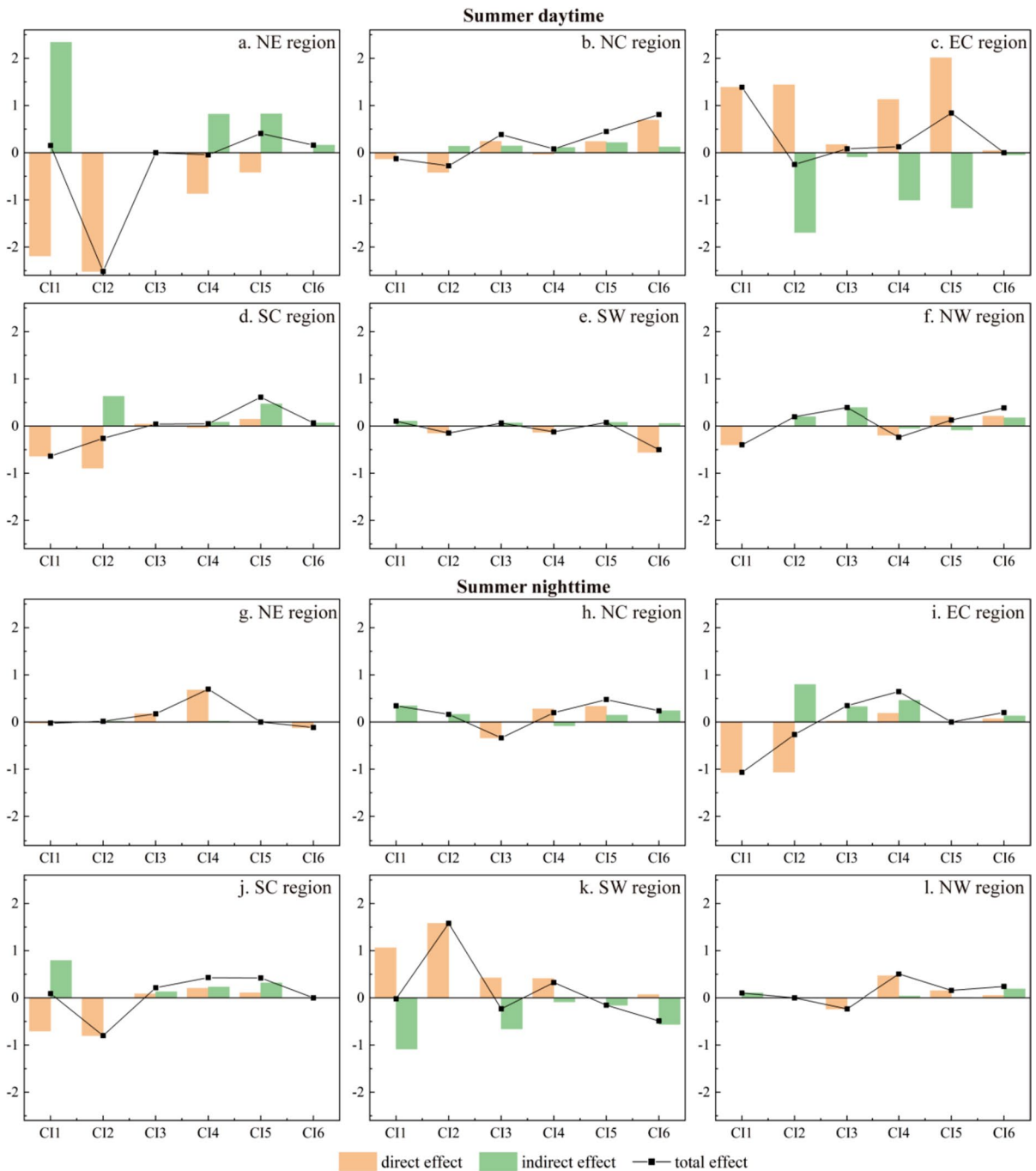


Fig. 7 The direct, indirect, and total effects of CIs of land use types on SUHII in six regions in summer daytime and nighttime. *Numbers adjacent to CIs represent land use types, 1: cropland; 2: forest; 3: grassland; 4: water bodies; 5: built-up land; 6: bare land

an indirect effect. The CIs of water bodies, built-up land, and bare land all exerted indirect effects through the CI of grassland. The direct effect from the CI of water bodies (0.467), and its indirect effect through

CI of cropland (0.039), had a total effect on SUHII of 0.506.

The complex effects of land use types' CIs on SUHII were both direct and indirect. The direct and

indirect effects in the same direction amplified the total effect. In contrast, positive and negative effects offset and reduced the magnitude of the total effect. During the daytime, the total effect of the CI of built-up land was positive in all regions; however, at nighttime, the CI of built-up land showed a negative total effect or no effect on SUHII in some regions (SW, NE, and EC). In the daytime, the CI of water bodies did not have the largest total effect on SUHII in any region, while in the nighttime, the CI of water bodies was the most influential factor in two regions (NW and NE). The total effect of the CI of water bodies was positive in all regions.

Discussion

Complex effects of LUCC on UHE

It is crucial to investigate the complex effects of CIs of LUCC, but existing knowledge about the regional-scale pathways through which LUCC impacts on UHE remains inadequate. To address this limitation, this study made assumption of all pathways through which the CIs directly and indirectly influenced SUHII. And then structural equation models for each of the six regions in China were constructed to verify the pathways in the assumption. The well-fitted direct and indirect pathways through which LUCC exerts regional effects on UHE were clarified, which is different from the previous studies (Li et al. 2017; Wu et al. 2021; Xiang et al. 2022). Previous studies have explored the relationships between LUCC and UHE based on land surface parameters or from the perspective of energy balance using SEM; however, this study paid greater attention to all land use types and their interactions (Li et al. 2017; Cao et al. 2021).

Our innovative attempt to decompose the complex effects of LUCC on UHE has the potential to further clarify the mechanisms via which LUCC impacts UHE. Based on the equations used to calculate CI and SUHII, the relationships among CIs of land use types and SUHII in each city were shown to be related to the LSTs of all land use types in that city. CI is the product of the LST difference between land use type and city and their area ratio (Supplementary Fig. S5). The LST difference determines whether the CI is positive or negative, and the area ratio represents the degree of influence of a given land use type on

the UHE. Moreover, the higher the area weight, the closer the LST of land use type and city will be. As shown in the base scenario and scenario 1 of Supplementary Fig. S6, although the area ratio of the same land use type is the same, the LST shows a considerable difference (e.g. daytime and nighttime of the same city), which can lead to differences in the warming or cooling effect of the same land use type on UHE. Additionally, the CIs of land use types undoubtedly cause the city's SUHII to differ. The comparison between the base scenario and scenario 1 reflects the static relationship of CIs exhibited by assuming LST changes as the areas of land use types remain stable. Further, it can be inferred to the dynamic relationship of CI resulting from assuming land use types' area changes during land use change. As shown in the base scenario and scenario 2 of Supplementary Fig. S6, the differences in area ratios and LSTs of land use types lead to significant differences in the CIs and SUHII (e.g. different cities at various stages of development). Overall, the mechanism via which the CIs of land use types directly impact SUHII arises from the difference in the nature and intensity of the human activities on the land (Chen et al. 2019; Qiao et al. 2023a). The indirect effect of the CI of one land use type on SUHII is derived from a chain reaction whereby the LST of the entire city and other land use types can be affected by that of one land use type (Huang et al. 2019; Hu and Li 2020). The direct and indirect effects of land use types' CIs on SUHII reflect inter-regional differences and demonstrate the innovation of application, which also has practical significance.

Differences and innovations from existing researches

In existing research, Huang et al. (2019) conducted an assessment for CIs of land use types in the City of Wuhan, China, Harmay et al. (2021) explored CIs of land use types in Melbourne, Australia. Although previous studies have explored a city or region in depth, they were still limited to fixed scales and lacked the geographical, climatic, and diurnal knowledge of land use type's CI at large scales. For example, both we and Huang et al. (2019) obtained that the CIs of cropland and forest in Wuhan in summer were less than 0, and the CI of built-up land was greater than 0. However, Huang et al. (2019) revealed that the CI of water bodies was less than 0, whereas we found that the CI of

water bodies in Wuhan was positive in the nighttime and negative in the daytime. The discussion on the diurnal contributing role of water bodies' CI will be continued in the next paragraph. Zhao et al. (2018) and Tarawally et al. (2018) assessed the CI of land use types at several time nodes and the CI did produce changes. However, the MK analysis conducted in the present study revealed the 15-year trend in CI more finely. Therefore, the present study filled the research gap of long time series analysis of CI at a large spatial scale.

In the present study, the CI of built-up land exerted positive total effects on SUHII in all regions in the daytime, as summarized in previous studies (Sun et al. 2016; Yu et al. 2022). It is necessary to emphasize the role of urban development boundaries in territory development planning (He et al. 2017; Hu et al. 2017; Xie et al. 2020). The CI values of water bodies in the present study were small. Furthermore, we discovered that a higher proportion of cities possessed negative CIs of water bodies during the day and positive CIs of water bodies at night. These results originated from the specific heat capacity of the water bodies (Kuang et al. 2015). As suggested by Huang et al. (2019), water bodies possess a high specific heat capacity and thus small temperature variation. And Brans et al. (2018) also found that the average temperature of water bodies was lower than the average temperature of the city during the daytime, and the opposite was true at night. In addition, the CI of forest in some cities also exhibited diurnal differences. For example, the CI of forests in Shennongjia of Hubei Province, and Da Hinggan Ling Prefecture of Heilongjiang Province, was positive at night and negative during the day. These two cities have in common a high proportion of forest area. At night, the stomata of tree leaves are closed and transpiration is reduced, while the closed forest canopy acts as an obstacle to the heat exchange in the near-surface layer, and the heat inside the forest is not easy to dissipate, resulting in the positive contribution of forest to UHE (Wang et al. 2023a, b). The positive and negative differences between daytime and nighttime CIs of the same land use type on UHE in the same city also verified the findings from Qiao et al (2013).

Decomposition of complex effects helps optimize the UHE from a landscape ecology perspective.

The total effects of land use types showed significant regional differences, and the dominant factor in SUHII varied regionally (Fig. 7). Previous studies have shown that water bodies and vegetation are key for mitigating UHE and that optimizing the landscape of water bodies and vegetation is crucial for reducing LST (Ayanlade and Jegede 2015; Hu and Li 2020; Wu et al. 2021). Nonetheless, it is important to recognize that not all geographical regions uniformly benefit from the direct cooling influences exerted by water bodies and vegetation on the UHE. In some cases, these cooling effects may be indirectly channeled through intermediary land use types, such as those denoted as EC region during the daytime (CI of forest indirectly influenced SUHII through CI of cropland while CI of water bodies indirectly through CIs of cropland and forest). It is worth underscoring that in specific geographical areas, notably in the context of NW region during the daytime, as well as NC and SW regions during the nighttime, water bodies and vegetation can paradoxically exhibit warming effects, either directly or indirectly. Moreover, when considering vegetation, it is crucial to acknowledge the considerable regional disparities in the roles that forest and grassland play as both sources and sinks of UHE within various landscapes (Chen et al. 2019; Wang et al. 2023a, b). The present study represents a regional and intraday refinement of the influences of land use types, thus has significance for city and regional sustainable development in terms of the long-term land services necessary for maintaining and improving human well-being (He et al. 2023; Wu 2013). The deterioration of UHE and the projected high frequency of extreme weather events will put more people at risk from heat-related threats (He et al. 2022; Qiao et al. 2023b). Enhancement of human well-being and the ability to respond to heat-safety events requires a close integration of sustainable management of land resources and increased resilience of cities (i.e., rational allocation of resources and the harmonious coexistence of human beings and nature) (Chen et al. 2020; Xie et al. 2020; Wang et al. 2023a, b).

Limitations and future research directions

The influence of LUCC on UHE has become a hotspot in landscape ecology research (Hu et al. 2017; Oke et al. 2017; Ding et al. 2021; Zhang et al. 2022).

This study provides potentially valuable ideas for examining the complex interactions between LUCC and UHE. However, the results should be interpreted in the context of certain limitations.

This study adopted a “bottom-up” analysis approach. CIs of six land use types and SUHII were calculated for the same cities, and then the factor calculation at the city scale was extended to the decomposition of complex effects at the regional scale. However, the more comprehensive analysis of the cause pathways of UHE on macroscopic scales should also consider socioeconomic development, population distribution, anthropogenic heat emission, atmospheric circulation, and feedbacks (Sun et al. 2016; Wu et al. 2023).

This study included trend tests on time series CI and SUHII during the period 2005–2019. Undoubtedly, the CIs and SUHII have changed over the last 15 years. However, the complex effects of LUCC on SUHII were only decomposed for 2019. 2019 was regarded as the closest situation to the present, with the aim of guiding current land use policies and urban management policies in China. Future work should extend the time to analyze the complex effects over long time series. It is also necessary to expand the study area to distinguish direct and indirect effects of land use types on SUHII in key global regions experiencing complex and dramatic climate change.

Conclusions

LUCC exerts essential effects on UHE. Previous studies have lacked long time series analysis of the CIs while also largely ignoring the indirect effects of land use types on SUHII, making it difficult to decompose the complex effects of CIs of land use types on SUHII. The present study has filled these research gaps and addressed important scientific questions utilizing the MK test, Sen’s slope estimator, and SEM, and thus has the potential to aid regional sustainable development and ecological civilization construction.

The results showed that 78.08% and 73.70% of the cities exhibited an increasing trend in SUHII during summer daytime and nighttime from 2005 to 2019, respectively. CI of built-up land mostly increased (> 50% of the cities in all regions showed significant increases). The most influential factors of SUHII in the daytime, namely CI of forest in the NE region

(−2.515) and CI of cropland in the SC (−0.637), EC (1.386), and NW (−0.399) regions, only had direct effects on SUHII. CI of bare land was the main factor directly and indirectly influencing SUHII in both the NC (0.810) and SW (−0.501) regions. At nighttime, CI of water bodies in the NW (0.506) and NE (0.697) regions, and CI of built-up land in the NC region, affected SUHII through both direct and indirect pathways. CI of forest in the SW (1.581) and SC (−0.800) regions, as well as CI of cropland in the EC region (−1.067), only had direct effects.

This study clarified the regional nature of LUCC-induced UHE by means of a bottom-up approach, thus expanding our ecological knowledge of CIs of land use types. Therefore, this study could help to reduce the negative effects of UHE, further achieve the SDGs, and fulfill cities’ roles in climate change prevention, mitigation, and adaptation.

Author contributions Conceptualization, TH and ZQ; Methodology, TH and ZQ; Software, TH, XX, and LL; Validation, LL, ZS, and DH; Formal Analysis, TH and YH; Investigation, NW and JC; Resources, XX; Data curation, TH; Writing—original draft, TH and ZQ; Writing—review and editing, ZQ, FW, and DH; Visualization, NW, JC, and YL; Funding acquisition, ZQ, FW, and XX. All authors have read and agreed to the published version of the manuscript.

Funding This research was funded by National Natural Science Foundation of China (Grant Numbers 52270187, 41971389, 41971233), Natural Science Foundation of Tianjin City (Grant Number 21JCYBJC00390), and the Major Projects of High-Resolution Earth Observation Systems of National Science and Technology (Grant Number 05-Y30B01-9001-19/20-4).

Data availability The MYD11A2 product for obtaining LST was from the official website of the National Aeronautics and Space Administration (<https://ladsweb.modaps.eosdis.nasa.gov>). LUCC was obtained from the global products of European Space Agency Climate Change Initiative Land Cover Project (<http://maps.elie.ucl.ac.be/CCI/viewer/index.html>). DEM was derived from the Resource and Environment Science and Data Center, Chinese Academy of Sciences (<http://www.resdc.cn>).

Declarations

Conflict of interest The authors have no relevant financial or non-financial interests to disclose.

Open Access This article is licensed under a Creative Commons Attribution 4.0 International License, which permits use, sharing, adaptation, distribution and reproduction in any medium or format, as long as you give appropriate credit to the original author(s) and the source, provide a link to the Creative Commons licence, and indicate if changes were made. The images or other third party material in this article are included

in the article's Creative Commons licence, unless indicated otherwise in a credit line to the material. If material is not included in the article's Creative Commons licence and your intended use is not permitted by statutory regulation or exceeds the permitted use, you will need to obtain permission directly from the copyright holder. To view a copy of this licence, visit <http://creativecommons.org/licenses/by/4.0/>.

References

- Ayanlade A, Jegede OO (2015) Evaluation of the intensity of the daytime surface urban heat island: how can remote sensing help? *Int J Image Data Fusion* 6(4):348–365
- Brans KI, Engelen JMT, Souffreau C, De Meester L (2018) Urban hot-tubs: local urbanization has profound effects on average and extreme temperatures in ponds. *Landsc Urban Plan* 176:22–29
- Cao Q, Liu YP, Georgescu M, Wu JG (2021) Impacts of landscape changes on local and regional climate: a systematic review. *Landsc Ecol* 35:1269–1290
- Chen XL, Zhao HM, Li PX, Yin ZY (2006) Remote sensing image-based analysis of the relationship between urban heat island and land use/cover changes. *Remote Sens Environ* 104(2):133–146
- Chen C, Park T, Wang XH, Piao SL, Xu BD, Chaturvedi RK, Fuchs R, Brovkin V, Ciais P, Fensholt R, Tommervik H, Bala G, Zhu ZC, Nemani RR, Myneni RB (2019) China and India lead in greening of the world through land-use management. *Nat Sustain* 2(2):122–129
- Chen GZ, Li X, Liu XP, Chen YM, Liang X, Leng JY, Xu XC, Liao WL, Qiu YA, Wu QL, Huang KN (2020) Global projections of future urban land expansion under shared socioeconomic pathways. *Nat Commun* 11(1):537
- Ding MZ, Yong B, Shen ZH, Yang ZK (2021) A methodology to quantitate the thermal influence of different land use types: a case study in Beijing, China. *Urban Clim* 40:101015
- Fu P, Weng QH (2016) A time series analysis of urbanization induced land use and land cover change and its impact on land surface temperature with Landsat imagery. *Remote Sens Environ* 175:205–214
- Harmay NSM, Kim D, Choi M (2021) Urban Heat Island associated with Land Use/Land Cover and climate variations in Melbourne Australia. *Sust Cities Soc* 69:102861
- He CY, Liu ZF, Xu M, Ma Q, Dou YY (2017) Urban expansion brought stress to food security in China: evidence from decreased cropland net primary productivity. *Sci Total Environ* 576:660–670
- He BJ, Wang JS, Zhu J, Qi JD (2022) Beating the urban heat: situation, background, impacts and the way forward in China. *Renew Sustain Energy Rev* 161:112350
- He T, Wang N, Tong YD, Wu F, Xu XL, Liu L, Chen JY, Lu YS, Sun ZY, Han DR, Qiao Z (2023) Anthropogenic activities change population heat exposure much more than natural factors and land use change: an analysis of 2020–2100 under SSP-RCP scenarios in Chinese cities. *Sustain Cities Soc* 96:104699
- Hou HR, Su HB, Liu K, Li XK, Chen SH, Wang WM, Lin JH (2022) Driving forces of UHI changes in China's major cities from the perspective of land surface energy balance. *Sci Total Environ* 829:154710
- Hu LQ, Li Q (2020) Greenspace, bluespace, and their interactive influence on urban thermal environments. *Environ Res Lett* 15(3):034041
- Hu XF, Zhou WQ, Qian YG, Yu WJ (2017) Urban expansion and local land-cover change both significantly contribute to urban warming, but their relative importance changes over time. *Landsc Ecol* 32(4):763–780
- Huang L, Zhai J, Sun CY, Liu JY, Ning J, Zhao GS (2018) Biogeophysical forcing of land-use changes on local temperatures across different climate regimes in China. *J Clim* 31(17):7053–7068
- Huang QP, Huang JJ, Yang XN, Fang CL, Liang YJ (2019) Quantifying the seasonal contribution of coupling urban land use types on Urban Heat Island using Land Contribution Index: a case study in Wuhan, China. *Sustain Cities Soc* 44:666–675
- IPCC (2021) Climate change 2021: the physical science basis. Contribution of Working Group I to the Sixth Assessment Report of the Intergovernmental Panel on Climate Change. Cambridge University Press, Cambridge
- Kuang WH, Liu Y, Dou Y, Chi W, Chen G, Gao C, Yang T, Liu J, Zhang R (2015) What are hot and what are not in an urban landscape: quantifying and explaining the land surface temperature pattern in Beijing, China? *Landsc Ecol* 30(2):357–373
- Lang W, Long Y, Chen TT (2018) Rediscovering Chinese cities through the lens of land-use patterns. *Land Use Policy* 79:362–374
- Li ZY, Wu WZ, Liu XH, Fath BD, Sun HL, Liu XC, Xiao XR, Cao J (2017) Land use/cover change and regional climate change in an arid grassland ecosystem of Inner Mongolia, China. *Ecol Model* 353:86–94
- Lu DM, Song KS, Zang SY, Jia MM, Du J, Ren CY (2015) The effect of urban expansion on urban surface temperature in Shenyang, China: an analysis with Landsat imagery. *Environ Model Assess* 20(3):197–210
- Mousivand A, Arsanjani JJ (2019) Insights on the historical and emerging global land cover changes: the case of ESA-CCI-LC datasets. *Appl Geogr* 106:82–92
- Oke TR, Mills G, Christen A (2017) Urban climates. Cambridge University Press, Cambridge
- Qiao Z, Tian GJ, Xiao L (2013) Diurnal and seasonal impacts of urbanization on the urban thermal environment: a case study of Beijing using MODIS data. *ISPRS J Photogramm Remote Sens* 85:93–101
- Qiao Z, Liu L, Qin YW, Xu XL, Wang BW, Liu ZJ (2020) The impact of urban renewal on land surface temperature changes: a case study in the main city of Guangzhou, China. *Remote Sens* 12(5):794
- Qiao Z, Lu YS, He T, Wu F, Xu XL, Liu L, Wang F, Sun ZY, Han DR (2023a) Spatial expansion paths of urban heat islands in Chinese cities: analysis from a dynamic topological perspective for the improvement of climate resilience. *Resour Conserv Recycl* 188:106680
- Qiao Z, Wang N, Chen JY, He T, Xu XL, Liu L, Sun ZY, Han DR (2023b) Urbanization accelerates urban warming by changing wind speed: evidence from China based on 2421 meteorological stations from 1978 to 2017. *Environ Impact Assess Rev* 102:107189

- Sun Y, Zhang XB, Ren GY, Zwiers FW, Hu T (2016) Contribution of urbanization to warming in China. *Nat Clim Change* 6(7):706–710
- Tarawally M, Xu WB, Hou WM, Mushore TD (2018) Comparative analysis of responses of land surface temperature to long-term land use/cover changes between a coastal and inland city: a case of Freetown and Bo Town in Sierra Leone. *Remote Sens* 10(1):112
- UCL-Geomatics (2017) Land cover CCI product user guide (version 2.0). https://www.esa-landcover-cci.org/?q=webfm_send/84. Accessed 20 May 2022
- UN (2018) World urbanization prospects: the 2018 revision. <https://www.un.org/development/desa/pd/news/world-urbanization-prospects-2018>. Accessed 16 Aug 2022
- Wan ZM (2014) New refinements and validation of the collection-6 MODIS land-surface temperature/emissivity product. *Remote Sens Environ* 140:36–45
- Wang N, Chen JY, He T, Xu XL, Liu L, Sun ZY, Qiao Z, Han DR (2023a) Understanding the differences in the effect of urbanization on land surface temperature and air temperature in China: insights from heatwave and non-heatwave conditions. *Environ Res Lett* 18:104038
- Wang Q, Wang XN, Meng Y, Zhou Y, Wang HT (2023b) Exploring the impact of urban features on the spatial variation of land surface temperature within the diurnal cycle. *Sustain Cities Soc* 91:104432
- Wu JG (2013) Landscape sustainability science: ecosystem services and human well-being in changing landscapes. *Landsc Ecol* 28(6):999–1023
- Wu JG (2019) Linking landscape, land system and design approaches to achieve sustainability. *J Land Use Sci* 14(2):173–189
- Wu W, Li LD, Li CL (2021) Seasonal variation in the effects of urban environmental factors on land surface temperature in a winter city. *J Clean Prod* 299:126897
- Wu CY, Li C, Ouyang LK, Xiao HR, Wu J, Zhuang MH, Bi X, Li JX, Wang CF, Song CH, Qiu T, Haase D, Hahs A, Finka M (2023) Spatiotemporal evolution of urbanization and its implications to urban planning of the megacity, Shanghai, China. *Landsc Ecol* 38(4):1105–1124
- Xi Y, Peng S, Liu G, Ducharme A, Ciais P, Prigent C, Li X, Tang X (2022) Trade-off between tree planting and wetland conservation in China. *Nat Commun* 13:1967
- Xiang Y, Ye Y, Peng CC, Teng MJ, Zhou ZX (2022) Seasonal variations for combined effects of landscape metrics on land surface temperature (LST) and aerosol optical depth (AOD). *Ecol Indic* 138:108810
- Xiao H, Kopecka M, Guo S, Guan YN, Cai DL, Zhang CY, Zhang XX, Yao WT (2018) Responses of urban land surface temperature on land cover: a comparative study of Vienna and Madrid. *Sustainability* 10(2):260
- Xie HL, Zhang YW, Zeng XJ, He YF (2020) Sustainable land use and management research: a scientometric review. *Landsc Ecol* 35(11):2381–2411
- Xu SL (2009) An approach to analyzing the intensity of the day-time surface urban heat island effect at a local scale. *Environ Monit Assess* 151(1–4):289–300
- Yang J, Wang YC, Xiao XM, Jin C, Xia JH, Li XM (2019) Spatial differentiation of urban wind and thermal environment in different grid sizes. *Urban Clim* 28:100458
- Yu WP, Shi JA, Fang YL, Xiang AM, Li X, Hu CH, Ma MG (2022) Exploration of urbanization characteristics and their effect on the urban thermal environment in Chengdu, China. *Build Environ* 219:109150
- Zawadzka JE, Harris JA, Corstanje R (2021) The importance of spatial configuration of neighbouring land cover for explanation of surface temperature of individual patches in urban landscapes. *Landsc Ecol* 36(11):3117–3136
- Zhang MM, Zhang C, Kafy AA, Tan SK (2022) Simulating the relationship between land use/cover change and urban thermal environment using machine learning algorithms in Wuhan City, China. *Land* 11(1):14
- Zhao HB, Zhang H, Miao CH, Ye XY, Min M (2018) Linking heat source–sink landscape patterns with analysis of urban heat islands: study on the fast-growing Zhengzhou city in central China. *Remote Sens* 10(8):1268
- Zhou WQ, Qian YG, Li XM, Li WF, Han LJ (2014) Relationships between land cover and the surface urban heat island: seasonal variability and effects of spatial and thematic resolution of land cover data on predicting land surface temperatures. *Landsc Ecol* 29(1):153–167
- Zhou DC, Xiao JF, Bonafoni S, Berger C, Deilami K, Zhou YY, Frolking S, Yao R, Qiao Z, Sobrino JA (2019) Satellite remote sensing of surface urban heat islands: progress, challenges, and perspectives. *Remote Sens* 11(1):48
- Zhou Y, Li XH, Liu YS (2020) Land use change and driving factors in rural China during the period 1995–2015. *Land Use Policy* 99:105048

Publisher's Note Springer Nature remains neutral with regard to jurisdictional claims in published maps and institutional affiliations.